

# BabyNet: A Lightweight Network for Infant Reaching Action Recognition in Unconstrained Environments to Support Future Pediatric Rehabilitation Applications

Amel Dechemi,<sup>1</sup> Vikarn Bhakri,<sup>1</sup> Ipsita Sahin,<sup>2</sup> Arjun Modi,<sup>2</sup> Julya Mestas,<sup>2</sup> Pamodya Peiris,<sup>1</sup> Danny Enriquez Barrundia,<sup>2</sup> Elena Kokkoni,<sup>2</sup> and Konstantinos Karydis<sup>1</sup>

**Abstract**— Action recognition is an important component to improve autonomy of physical rehabilitation devices, such as wearable robotic exoskeletons. Existing human action recognition algorithms focus on adult applications rather than pediatric ones. In this paper, we introduce BabyNet, a light-weight (in terms of trainable parameters) network structure to recognize infant reaching action from off-body stationary cameras. We develop an annotated dataset that includes diverse reaches performed while in a sitting posture by different infants in unconstrained environments (e.g., in home settings, etc.). Our approach uses the spatial and temporal connection of annotated bounding boxes to interpret onset and offset of reaching, and to detect a complete reaching action. We evaluate the efficiency of our proposed approach and compare its performance against other learning-based network structures in terms of capability of capturing temporal inter-dependencies and accuracy of detection of reaching onset and offset. Results indicate our BabyNet can attain solid performance in terms of (average) testing accuracy that exceeds that of other larger networks, and can hence serve as a light-weight data-driven framework for video-based infant reaching action recognition.

## I. INTRODUCTION

Identifying human motor actions that emerge early in life (e.g., spontaneous movements of arms and legs, kicking, crawling, etc.) is an emerging vision-based action recognition research direction [1]–[3]. The ability to automate the process of detecting, recognizing, and classifying actions performed by young children and infants from visual data can prove useful across applications. Examples include monitoring for safety [4]–[6], studying infants’ interaction with caregivers [7], identifying markers for diagnosis of neuromotor disorders [1], [2], [8]–[10], as well as—primarily of interest herein—closing action-perception loops for smart environments and assistive wearable robotic devices [11]–[15].

Developing algorithms to accurately and reliably recognize infant motor actions is not straightforward. There is inherent movement variability within and across young humans as a natural result of learning and growth [16]. For example, the kinematic properties of infant reaching (the motor action of interest in this paper) change over the first few years as infants learn how to adapt to environmental, task, and biomechanical constraints [17], [18]. In fact, it may take years for children to achieve smooth and straight reaching

trajectories similar to those seen in adults [19], [20]. Thus, existing skeletal models or learning-based pose estimation methods often used in adult action recognition may not fit well in pediatric action recognition [4], [11], [21].

State-of-the-art adult action recognition methods require very large training datasets [22]–[27]. Because of protection of privacy of minors, and given that data from adult activities can be used in a wider range of applications compared to infant activities, there is a lack of infant activity datasets. A few notable exceptions exist [3], [28], [29]; however, these datasets do not apply in this work that specifically targets infant reaching. We focus on reaching as it is one of the earliest motor milestones leading to environment exploration and learning, and hence, advancing reaching is an important goal in pediatric rehabilitation [30], [31]. In this context, vision-based reaching action recognition may guide autonomous reasoning regarding the amount of passive/active feedback that assistive upper extremity devices may provide to the pediatric user [15].

This paper has a twofold aim. First, to develop a new dataset focusing on infant reaching. Second, to use the dataset to develop a machine learning algorithm for infant reaching action recognition. The dataset is constructed based on diverse online-shared videos that demonstrate reaching actions of both typically-developing infants as well as infants with arm mobility challenges (all between 6–12 months of age). Annotations and bounding boxes that describe reaching properties (e.g., reaching onset/offset, object touched, arm position in beginning/end of reach, etc.) are also included. Next, BabyNet, a new network structure aimed at infant reaching action recognition is developed. The network is built upon a long short-term memory (LSTM) module to model different stages of reaching action through a spatial-temporal interpretation. Our motivation is to provide a light-weight (based on the number of trainable parameters) structure of comparable efficiency with (significantly) larger ones.

Succinctly, the contributions of this paper include:

- A new dataset for infant reaching action recognition including action annotations and bounding boxes.
- A light-weight network BabyNet able to model short-range and long-range motion dependencies of the different stages of infant reaching action.
- Performance validation and comparison of BabyNet against other learning-based methods using our dataset.

<sup>1</sup> Dept. of Electrical and Computer Engineering, University of California, Riverside. Email: {adech003, vbhak001, ppeir002, karydis}@ucr.edu.

<sup>2</sup> Dept. of Bioengineering, University of California, Riverside. Email: {isahi001, amodi003, jmest001, denri013, elena.kokkoni}@ucr.edu.

## II. RELATED WORKS

### A. Overview of Human Action Recognition Approaches

State-of-the-art video-based human action recognition algorithms have been steadily shifting from the use of Support Vector Machines or Hidden Markov models (e.g., [32], [33]) to the use of deep learning networks, primarily due to the accessibility, adaptability, accuracy and decrease in time execution the latter can offer (e.g., [34]–[37]). One of the first significant attempts [34] used two separated convolutional neural networks (CNNs) trained to extract features from a sampled RGB video frame paired with the surrounding stack of optical flow images. As optical flow is computationally expensive and has a burdensome optimization process, most follow-on works used a CNN to learn the optical flow prediction [38], [39], thus reducing the number of parameters as only one network is needed. Other methods explored the advantages of LSTM structures [37] to incorporate motion by updating the pooling of the features across time [40], [41].

Despite some remarkable results achieved by RGB-video-based methods to date, some key challenges remain. These include, for example, background clutter, illumination disparity, pose/viewpoint variation, to name a few. One way to improve recognition performance under these challenges is via skeleton data representations that do not contain color information. Early relevant works did not use information regarding internal dependencies between body joints [42]–[45]; more recent works apply graph convolutional networks to extract features by building a skeleton graph composed of vertices and edges to represent joints and links, respectively [46]–[48]. These approaches rely on datasets that contain mostly motion actions performed by adults [22]–[27].

### B. Action Recognition for Rehabilitation Purposes

Action recognition algorithms can contribute to the field of rehabilitation through their integration in the automation of assistive devices and for assessment of training outcomes. A recent paradigm shift seeks to develop technology and perform training in the real world to increase dosage and help translate better the effects of training [49], [50]. Infants, in particular, learn from exposure to complex (unconstrained) and variable environments, as well as in the presence of immediate rewards and constant motivation as they perform motor tasks in such environments. However, taking training outside of the lab or clinic poses various challenges, such as timely and accurate outcome evaluation, and in many cases, absence of a rehabilitation expert. Related works tend to use virtual reality or camera-based systems [51]–[54] in support of training in such settings.

Specifically in the context of pediatric rehabilitation, recent paradigms involve action recognition methods to make interaction with assistive technology more efficient and effective [3], [11]–[13], [55]. For example, social humanoid robots assist in non-contact upper-limb rehabilitation autonomously, by performing a set of prescribed arm-poses for a child to imitate [55]. Movements here are captured by a Kinect depth camera, stored as 3D skeletons and then compared with entries from a knowledge base. Other applications

use multiple cameras to alleviate issues such as occlusions that are more likely to happen in sessions involving young children [3], [11]–[13]. For example, Kokkoni et al. [13] developed a learning environment for infants using socially-assistive robots and body weight support technology. Kinect cameras were utilized to capture movement, and action recognition algorithms were developed to close the loop between the infants and the robots [3], [13]. Our proposed action recognition work is in line with the aforementioned approaches but for use with a different type of technology; our future goal is to use reaching action recognition to automate our wearable upper extremity device for infants so as to provide passive/active feedback during reaching [15].

## III. METHODS

### A. Dataset of Infant Reaching Actions

Videos were collected from the YouTube<sup>TM</sup> online video-sharing platform using search terms such as ‘infant,’ ‘reaching,’ ‘grabbing,’ and ‘sitting.’ Videos were included in the dataset if they displayed awake and behaving infants: (1) up to 12 months of age, (2) placed in a sitting position, (3) reaching for objects (regardless of shape and/or position), (4) performing at least one reaching action during which the camera remained stationary, and (5) performing at least one reaching action during which both hand and object were fully visible. Both typically-developing infants and infants with arm mobility challenges were considered. The majority of videos were recorded in natural (unconstrained) environments (e.g., family’s home, clinic). The clothes of infants, presented objects, and the background varied from video to video. Figure 1 shows some illustrative samples.

A total of 193 reaches performed by 21 distinct subjects were collected through 20 videos (Table I).<sup>1</sup> In most cases, the video description was detailing the age and gender of the subject; in a few exceptions that this information was omitted (entries marked with an \* in Table I), our research team empirically estimated these characteristics. Out of the 21 subjects, five subjects had a medical diagnosis (four with Down syndrome and one with congenital anomaly; information was provided in the video description). Each subject was assigned a unique identification number.

Videos were processed by an open-source software (www.kinovea.org) to obtain annotations of the Reaching Onset (RN) and the Reaching Offset (RF) of every reaching action in all videos. RN was defined as the first frame in which the infant’s hand (left, right, or both) started moving toward the presented object. RF was defined as the first frame in which the infant’s hand intentionally touched the object (Figure 2). Hand-to-hand object transfers, partial (interrupted or unfinished) reaching actions, and actions containing frames where the hand and/or object were occluded, were excluded from further analyses in this paper.

Action annotation analyses were conducted by four researchers of our team. These four researchers first went through a separate protocol to establish reliability. Reaching

<sup>1</sup>Video handling procedures were according to YouTube’s statement on fair use of videos for research purposes.



Fig. 1. Examples of frames from the dataset.

TABLE I  
SUBJECTS AND ANNOTATED REACHES/OBJECTS PER SUBJECT.

Subject ID	Age [months]	Gender [M/F]	# Reaches			Total Obj.
			LH	RH	Total	
T01	6-8	F	5	3	8	4
T02	8-10	M	8	4	12	4
T03	11-12*	M	2	8	10	2
T04	6-12	F	3	5	8	5
T05	10-12	M*	3	1	4	2
T06	10-12	M*	0	2	2	2
T07	6-7*	M	2	3	5	3
T08	<12*	M	4	5	9	1
T09	6	F	3	6	9	2
T10	6	F	3	3	6	3
T11	6-8	M	2	1	3	2
T12	8	F	16	33	49	8
T13	10	F	5	9	14	5
T14	6	F	1	1	2	2
T15	9	M	20	20	40	10
T16	7	F	2	1	3	2
<hr/>						
D01	6-9	F	1	-	1	1
D02	10	M	-	1	1	1
D03	<12*	M	4	1	5	1
D04	9-12	M	1	-	1	1
D05	<12*	M	1	-	1	1
Total	-	-	86	107	193	57

actions from two sample videos were initially annotated by all four researchers. Only when they all achieved a 100% agreement on the frequency of reaching actions and a +/- 3 frame selection difference between RN and RF, they proceeded with analysis of the remaining videos (two researchers assigned per remaining video).



Fig. 2. Sample annotated Reaching Onset (left) and Offset (right) frames.

The annotation process resulted in a total of 193 reaches with 86 reaches performed by the left hand (LH) and 107 by the right hand (RH) and 57 different objects involved in the reaching action (see Table I). The stage of motor development each subject is at affects both the quality of reaching actions as well as their length. Figure 3 depicts the distribution of the duration of all reaches in our dataset. The large variability of reaching action duration can be readily observed, though the majority last between 5-15 frames.

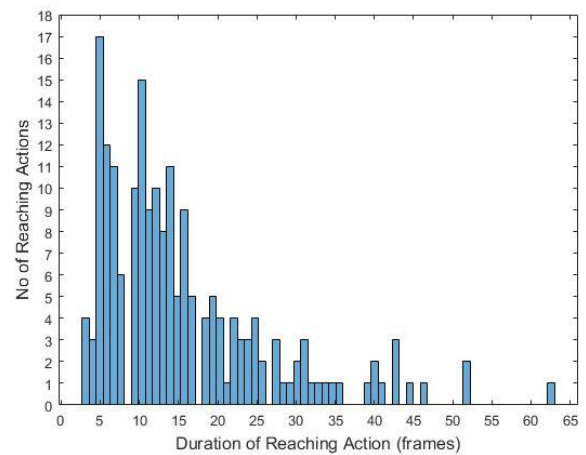


Fig. 3. Distribution of reaches duration frequencies.

## B. Annotation of Bounding Boxes

To assess the spatial and temporal connection during the reaches, we employed detection of each of the hands (LH, RH) and any object(s) on each frame using bounding boxes. Two researchers of the team annotated 607 images randomly

sampled out of total of 2,984 frames for the complete dataset. For each frame, we created bounding boxes of the infant, their left hand, their right hand, and the objects involved in the reaching action. Annotation of the selected 607 frames resulted in a total of 3,194 bounding boxes.

Using the sampled images and corresponding bounding boxes we trained an object detector to help automate the process for the remaining frames. We started with a pre-trained YOLOv3 object detector [56] with the COCO dataset [57], which we then finetuned with our obtained annotations. During finetuning, four categories were registered for the detector: infant, left hand (LH), right hand (RH) and object. The object detector was trained and tested using a 75% (training) / 25% (testing) split.

### C. Baseline Approaches for Comparison

We considered four baseline network structures to serve as the basis to evaluate our proposed structure's performance.

- Multi-Layer Perceptron (MLP). We trained a four-layer network with two inputs and four outputs.
- ResNet. Starting with a pretrained ResNet-50 model [58], the last Bottleneck block in the fourth layer of the network was retrained along with the fully connected layer in an effort to examine if overfitting can be avoided.
- ResNet+LSTM. An LSTM block was integrated after the average pooling layer of the final residual block of the aforementioned ResNet-50 model in an effort to examine if temporal correlation features of reaching actions can be captured.
- LSTM with Optflow (O-LSTM). A single-layer LSTM with 50% dropout was trained to leverage the information provided by the optical flow images.

All models except for O-LSTM use RGB images of size 224x224 directly as inputs and were evaluated on our dataset and were trained with learning rate 0.001 using Adam optimizer and cross entropy loss. Both ResNet and ResNet+LSTM model were evaluated with the data augmentation by altering randomly the images through techniques including shift, scale and rotation. The O-LSTM uses optical flow images obtained with the Farneback method [59] and trained with a learning rate of 0.0001 using Adam optimizer and cross entropy loss and inputs of a flattened image of size 1x12,288 (from a reduced-size 64x64 RGB source image) to reduce the training time.

### D. The Proposed BabyNet Algorithm

The flow chart of our proposed algorithm for infant reaching action recognition (BabyNet) is depicted in Figure 4. Given sequence of  $T$  video frames, let  $X = \{x_i^{T_i}\}$  and  $H = \{h_{L,R}^{T_i}, h_{R,L}^{T_i}\}$  denote the objects and left and right hands detected in the frame sequence, respectively. Note that we did not incorporate any tracking information, but instead we relied on the centers of the bounding boxes as the main source of information regarding the hands' and objects' locations on the image. The coordinates of the bounding boxes were acquired through object detection along with the labels for

each frame  $T_i$ . The two keyframes, TRN for the onset and TRF for the offset, are initialized at the first frame. To enable spatial-temporal reasoning between  $X$  and  $H$ , we elected to split a reaching action into two distinct phases: onset and offset. Each phase was detected through a separate process.

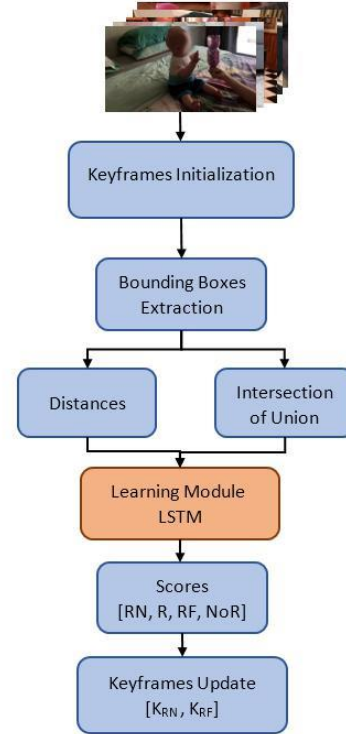


Fig. 4. The underlying process followed by our proposed BabyNet network for infant reaching action recognition.

1) The Reaching Onset Phase: Using the coordinates of the bounding boxes, we can first compute the distance  $d_j^i$  between the hands  $\{h_{L,R}^{T_j}, h_{R,L}^{T_j}\}$  and the object  $x_i$  in  $X$  in the current frame  $T_j$ . When  $d_j^i - d_{j-1}^i < 0$ , the onset detection remains valid and hence TRN can be kept as a keyframe. When  $d_j^i - d_{j-1}^i \geq 0$  and that positive increase continues for four consecutive frames, the onset is invalidated and  $T_i$  can be set as the new keyframe TRN. This approach can help avoid false negatives during this phase.

2) The Reaching Offset Phase: The intersection of union (IOU) between the hands  $\{h_{L,R}^{T_j}, h_{R,L}^{T_j}\}$  and the object  $x_i$  can be estimated and compared to a threshold value determined through the learning process. If the IOU is less than the threshold, no offset will be detected and the keyframe TRF can be definitively set as  $T_i$ . Otherwise, the keyframe is updated as  $T_i$  until the next frame.

3) Core Structure of BabyNet: Our proposed BabyNet uses the LSTM structure to learn the relation between the bounding boxes through the input consisting of the distances and intersection of union (IOU). The output is the scores for onset (RN), offset (RF), reach (R) and no reach (NoR) are used to update identified keyframes. The reach (R) is the label used for all frames between the onset RN and offset RF frames. Similarly, the no reach (NoR) is the label for all frames before the onset and after the offset.

TABLE II  
COMPARATIVE RESULTS OF THE PERFORMANCE THE NETWORK STRUCTURES CONSIDERED IN THIS WORK.

Model	Parameters (Trainable)/(Total)	Avg. Training Accuracy [%]	Avg. Validation Accuracy [%]	Avg. Testing Accuracy [%]	Precision NoR / R	Recall NoR / R
ResNet						
No Data Augm.	4,468,739 / 23,514,179	98.30	50.61	53.43	0.65 / 0.40	0.55 / 0.51
ResNet						
With Data Augm.	4,468,739 / 23,514,179	94.59	53.65	58.16	0.68 / 0.45	0.62 / 0.52
ResNet+LSTM						
No Data Augm.	9,186,819 / 28,232,259	98.61	50.59	54.21	0.65 / 0.41	0.57 / 0.49
ResNet+LSTM						
With Data Augm.	9,186,819 / 28,232,259	94.31	54.53	54.42	0.68 / 0.42	0.51 / 0.60
O-LSTM	117,460,994 / 117,460,994	75.44	81.16	63.71	0.59 / 0.82	0.92 / 0.35
MLP	144 / 144	47.66	46.13	51.8	0.55 / 0.67	0.78 / 0.42
BabyNet (Ours)	1,204 / 1,204	44.45	38.93	66.27	0.57 / 0.66	0.72 / 0.49

4) Implementation Details: BabyNet has two inputs ( $T = 2$ ) and four outputs (RN, RF, NoR, R). Preliminary testing showed that selecting  $T = 2$  can improve temporal correlation predictions without overfitting. BabyNet was trained with learning rate 0.001 using Adam optimizer and cross entropy loss. In initial testing we used a small dataset of 63 reaches with a 60% training, 15% validation, and 25% testing split. While BabyNet (and MLP) can perform well with small datasets (as desired), larger structures (ResNet variants and O-LSTM) were found to overfit the dataset. To resolve this issue, we tested larger networks with the full dataset (193 reaches) while keeping BabyNet and MLP at 63 reaches.

#### IV. RESULTS

Comparison results, including classification accuracy (range: [0–100%]) and precision/recall scores (range: [0–1]), are shown in Table II. Including the precision/recall scores of both no reaches (NoR) and reaches (R) serves a dual purpose:

- (1) to examine the trade-off between different methods; and
- (2) to help attain a more clear distinction in terms of the structures' capability to correctly differentiate between no reaches and reaches.

We first compared the performance of the family of ResNet and ResNet+LSTM structures. The ResNet structure with data augmentation achieves the best performance with an average testing accuracy of 58.16%. With reference to Table II, we can observe that the models with data augmentation give nearly the same results as with those without data augmentation (cf. 58.16% to 53.43% in ResNet and 54.42% to 54.21% in ResNet+LSTM). To properly gauge the effect of data augmentation on accuracy, we compared the trade-off between precision and recall of the two networks. The ResNet model with data augmentation has higher precision along with the ResNet+LSTM model with data augmentation. However, the recall score is slightly different as the ResNet structure with data augmentation achieved 0.62 for no reaches (NoR) and 0.52 for reaches (R) which indicates

that the number of false negatives is lower for the no reaches (NoR) cases. In contrast, the ResNet+LSTM with data augmentation had a recall of 0.51 for no reaches and 0.60 for reaches, thus leading to a lower number of false negatives for the case of reaches (Table II).

Results of the O-LSTM trained with optical flow images show that this structure can achieve 63.71% of average testing accuracy, surpassing all ResNet-based structures. In terms of precision and recall, the model has lower false positive detection for reaches (R) detection than no reaches (NoR) ones (cf. 0.59 to 0.82), but these detections are more likely to be false negatives in the case of reaches (given the recall score of 0.35)—it was a challenge to learn to recognize short reaches. O-LSTM requires a significantly larger number of parameters since the input optical flow image needs to be flattened (i.e. transform from a size of  $3 \times 64 \times 64$  to  $1 \times 12,288$ ). This is in addition to the necessary pre-processing (high) computational effort required to transform the original RGB image to optical flow image (see Figure 5).

Results demonstrate that our proposed BabyNet outperforms all structures in terms of average testing accuracy while using the second smallest number of parameters and the small dataset of 63 reaches and in spite of featuring lower average training/validation accuracy. The observed lower validation accuracy can be explained by the fact that more challenging reaches were included in the validation set which, nevertheless, did not impact the ability of BabyNet to learn pertinent features. The observed lower training accuracy can be associated with the reduced training dataset size, whereby training accuracy would keep improving with more data. Still, BabyNet can perform well (in terms of testing accuracy) despite sub-optimal training.

The MLP structure is the smallest one (also uses 63 reaches), but it has the worst average testing accuracy (see Table II). Furthermore, both networks predicted the same number of frames incorrectly during the reach phase but the MLP predicted 20 frames incorrectly during the no

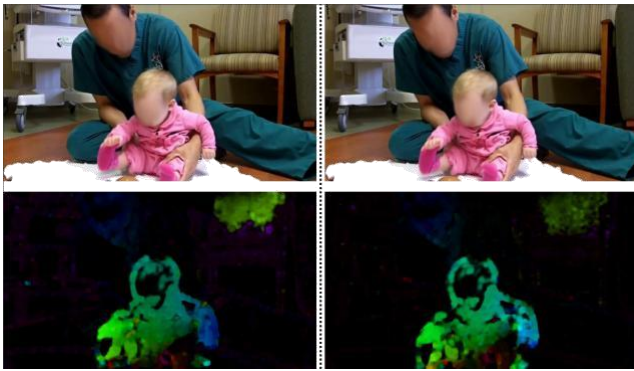


Fig. 5. RGB (top panels) and equivalent optical flow images (bottom panels) spaced two frames apart (from left to right). Optical flow images can capture more clearly small and subtle changes, but at a (significant) pre-processing computational cost compared to plain RGB image inputs.

reach action whereas BabyNet only predicted six frames incorrectly. In term of keyframes, BabyNet only had a delay of one frame while predicting the reach whilst the MLP had a delay of four frames. In contrast, the MLP was not able to learn the motion of the reaching action, and had difficulties to discern the transition from a reach to a no reach.

## V. DISCUSSION AND CONCLUSIONS

The paper proposed a new light-weight network called BabyNet aimed at infant reaching action recognition. Our approach was found able to model short-range and long-range motion correlation of different key phases of a reaching action: its onset and offset. To develop the network and evaluate its performance, we also developed a dataset specifically suitable for infant action recognition that includes action and bounding box annotations.

Evaluation results demonstrated that our proposed BabyNet is small yet powerful, and can challenge the performance of significantly larger structures by achieving 66.27% average testing accuracy (the highest one) on our dataset. The family of Resnet-based structures, despite their solid performance during training and validation, were found to provide results with increased false positives rates. On the other hand, the O-LSTM (that has the second best average testing accuracy and comparable to BabyNet's) could not balance between no reaches (NoR) and reaches (R)—recall rates of 0.92 and 0.35, respectively. Yet, it remains an approach worth of further investigation in future work due to the ability of optical flow images to better differentiate subtle motion patterns compared to RGB images (see Figure 5).

Compared to the MLP (which is of comparable size to BabyNet), our BabyNet performed much better (approximately 27% improved performance) with almost the same precision/recall scores. However, it provides onset and offset keyframes at precision of one frame while the MLP had a delay of 4 frames. These promising findings demonstrate that BabyNet can serve as a light-weight data-driven framework for video-based infant reaching action recognition.

As this stage, BabyNet can be challenged by the lack of viewpoint variation in the dataset and reliance on the performance of the detector network; missing detection of the

hands and/or the object can undermine reaching action recognition. Future work aims to extend the dataset introduced herein to help generalize to reaching action in other postures. As mentioned above, these efforts gear toward the implementation and assessment of the BabyNet's performance in closing the action-perception loop in our upper extremity pediatric wearable robotic device under development [15].

## REFERENCES

- [1] C. Chambers, N. Seethapathi, R. Saluja, H. Loeb, S. Pierce, D. Bogen, L. Prosser, M. J. Johnson, and K. P. Kording, "Computer vision to automatically assess infant neuromotor risk," *IEEE Trans. on Neural Systems and Rehabilitation Engineering*, vol. 28, no. 11, pp. 2431–2442, 2020.
- [2] V. Emeli, K. E. Fry, and A. Howard, "Towards Infant Kick Quality Detection to Support Physical Therapy and Early Detection of Cerebral Palsy: A Pilot Study," in *IEEE Int. Conf. on Robot and Human Interactive Communication*, 2020, pp. 1069–1074.
- [3] C. Pacheco, E. Mavroudi, E. Kokkoni, H. G. Tanner, and R. Vidal, "A detection-based approach to multiview action classification in infants," in *Int. Conf. on Pattern Recognition*, 2021, pp. 6112–6119.
- [4] S. Suzuki, Y. Mitsukura, H. Igarashi, H. Kobayashi, and F. Harashima, "Activity recognition for children using self-organizing map," in *IEEE Int. Symp. on Robot and Human Interactive Communication*, 2012, pp. 653–658.
- [5] J. Goto, T. Kidokoro, T. Ogura, and S. Suzuki, "Activity recognition system for watching over infant children," in *IEEE Int. Symp. on Robot and Human Interactive Communication*, 2013, pp. 473–477.
- [6] Q. Nie, X. Wang, J. Wang, M. Wang, and Y. Liu, "A child caring robot for the dangerous behavior detection based on the object recognition and human action recognition," in *IEEE Int. Conf. on Robotics and Biomimetics*, 2018, pp. 1921–1926.
- [7] L. Klein, V. Ardulov, Y. Hu, M. Soleymani, A. Gharib, B. Thompson, P. Levitt, and M. J. Mataric, "Incorporating Measures of Intermodal Coordination in Automated Analysis of Infant-Mother Interaction," in *Int. Conf. on Multimodal Interaction*, 2020.
- [8] T. L. Westeyn, G. D. Abowd, T. E. Starner, J. M. Johnson, P. W. Presti, and K. A. Weaver, "Monitoring children's developmental progress using augmented toys and activity recognition," *Personal and Ubiquitous Computing*, vol. 16, pp. 169–191, 2011.
- [9] A. Stahl, C. Schellewald, Ø. Stavdahl, O. M. Aamo, L. Adde, and H. Kirkerød, "An optical flow-based method to predict infantile cerebral palsy," *IEEE Trans. on Neural Systems and Rehabilitation Engineering*, vol. 20, no. 4, pp. 605–614, 2012.
- [10] J. Hashemi, M. Tepper, T. Vallin Spina, A. Esler, V. Morellas, N. Papanikolopoulos, H. Egger, G. Dawson, and G. Sapiro, "Computer vision tools for low-cost and noninvasive measurement of autism-related behaviors in infants," *Autism research and treatment*, vol. 2014, 2014.
- [11] N. Efthymiou, P. Koutras, P. P. Filintisis, G. Potamianos, and P. Maragos, "Multi-view fusion for action recognition in child-robot interaction," in *IEEE Int. Conf. on Image Processing*, 2018, pp. 455–459.
- [12] A. Tsiami, P. Koutras, N. Efthymiou, P. P. Filintisis, G. Potamianos, and P. Maragos, "Multi3: Multi-sensory perception system for multimodal child interaction with multiple robots," in *IEEE Int. Conf. on Robotics and Automation*, 2018, pp. 4585–4592.
- [13] E. Kokkoni, E. Mavroudi, A. Zehfroosh, J. C. Galloway, R. Vidal, J. Heinz, and H. G. Tanner, "Gearing smart environments for pediatric motor rehabilitation," *Journal of NeuroEngineering and Rehabilitation*, vol. 17, no. 1, 2020.
- [14] E. Marinoiu, M. Zanfir, V. Olaru, and C. Sminchisescu, "3d human sensing, action and emotion recognition in robot assisted therapy of children with autism," in *IEEE/CVF Conf. on Computer Vision and Pattern Recognition*, 2018, pp. 2158–2167.
- [15] E. Kokkoni, Z. Liu, and K. Karydis, "Development of a Soft Robotic Wearable Device to Assist Infant Reaching," *Journal of Engineering and Science in Medical Diagnostics and Therapy*, vol. 3, no. 2, pp. 1–9, 2020.
- [16] L. Fetters, "Perspective on variability in the development of human action." *Physical therapy*, vol. 90, no. 12, pp. 1860–7, 12 2010.
- [17] J. Konczak and J. Dichgans, "The development toward stereotypic arm kinematics during reaching in the first 3 years of life," *Experimental Brain Research*, vol. 117, no. 2, pp. 346–354, 1997.

- [18] E. Thelen, D. Corbetta, K. Kamm, J. P. Spencer, K. Schneider, E. Thelen, D. Corbetta, K. Kamm, J. P. Spencer, and K. Schneider, "The Transition to Reaching: Mapping Intention and Intrinsic Dynamics." *Child development*, vol. 64, no. 4, pp. 1058–1098, 1993.
- [19] N. E. Berthier and R. Keen, "Development of reaching in infancy," *Experimental Brain Research*, vol. 169, no. 4, pp. 507–518, 2006.
- [20] S. Schneiberg, H. Sveistrup, B. McFadyen, P. McKinley, and M. F. Levin, "The development of coordination for reach-to-grasp movements in children," *Experimental Brain Research*, vol. 146, no. 2, pp. 142–154, 2002.
- [21] G. Sciortino, G. M. Farinella, S. Battiato, M. Leo, and C. Distanto, "On the estimation of children's poses," in *Int. Conf. on Image Analysis and Processing*. Springer, 2017, pp. 410–421.
- [22] K. Soomro, A. R. Zamir, and M. Shah, "Ucf101: A dataset of 101 human actions classes from videos in the wild," *ArXiv*, vol. abs/1212.0402, 2012.
- [23] J. Carreira and A. Zisserman, "Quo vadis, action recognition? a new model and the kinetics dataset," in *IEEE/CVF Conf. on Computer Vision and Pattern Recognition*, 2017, pp. 6299–6308.
- [24] H. Kuehne, H. Jhuang, E. Garrote, T. Poggio, and T. Serre, "Hmdb: A large video database for human motion recognition," in *IEEE Int. Conf. on Computer Vision*, 2011, pp. 2556–2563.
- [25] A. Shahroudy, J. Liu, T.-T. Ng, and G. Wang, "Ntu rgb+d: A large scale dataset for 3d human activity analysis," in *IEEE/CVF Conf. on Computer Vision and Pattern Recognition*, 2016, pp. 1010–1019.
- [26] D. Damen, H. Doughty, G. Maria Farinella, S. Fidler, A. Furnari, E. Kazakos, D. Moltisanti, J. Munro, T. Perrett, W. Price, and M. Wray, "Scaling egocentric vision: The epic-kitchens dataset," in *European Conf. on Computer Vision*, 2018, pp. 720–736.
- [27] R. Goyal, S. E. Kahou, V. Michalski, J. Materzynska, S. Westphal, H. Kim, V. Haenel, I. Fruend, P. Yianilos, M. Mueller-Freitag, F. Hoppe, C. Thureau, I. Bax, and R. Memisevic, "The "something something" video database for learning and evaluating visual common sense," in *IEEE Int. Conf. on Computer Vision*, 2017, pp. 5842–5850.
- [28] N. Hesse, C. Bodensteiner, M. Arens, U. G. Hofmann, R. Weinberger, and A. Sebastian Schroeder, "Computer vision for medical infant motion analysis: State of the art and RGB-D data set," in *European Conf. on Computer Vision Workshops*. Springer, 2018, pp. 32–49.
- [29] N. Hesse, S. Pujades, J. Romero, M. J. Black, C. Bodensteiner, M. Arens, U. G. Hofmann, U. Tacke, M. Hadders-Algra, R. Weinberger, W. Muller-Felber, and A. S. Schroeder, "Learning an infant body model from rgb-d data for accurate full body motion analysis," in *Int. Conf. on Medical Image Computing and Computer-Assisted Intervention*. Springer, 2018, pp. 792–800.
- [30] M. A. Lobo and J. C. Galloway, "The onset of reaching significantly impacts how infants explore both objects and their bodies," *Infant Behavior and Development*, vol. 36, no. 1, pp. 14–24, 2013.
- [31] M. Lobo, J. Galloway, and J. C. Heathcock, "Characterization and intervention for upper extremity exploration & reaching behaviors in infancy," *Journal of Hand Therapy*, vol. 28, no. 2, pp. 114–125, 2015.
- [32] C. Schuldt, I. Laptev, and B. Caputo, "Recognizing human actions: a local svm approach," in *Int. Conf. on Pattern Recognition*, 2004, pp. 32–36.
- [33] J. Gu, X. Ding, S. Wang, and Y. Wu, "Action and gait recognition from recovered 3-d human joints," *IEEE Trans. on Systems, Man, and Cybernetics, Part B (Cybernetics)*, vol. 40, no. 4, pp. 1021–1033, 2010.
- [34] K. Simonyan and A. Zisserman, "Two-stream convolutional networks for action recognition in videos," in *Conf. on Neural Information Processing Systems*, 2014, pp. 568–576.
- [35] L. Wang, Y. Xiong, Z. Wang, Y. Qiao, D. Lin, X. Tang, and L. Van Gool, "Temporal segment networks: Towards good practices for deep action recognition," in *European Conf. on Computer Vision*. Springer, 2016, pp. 20–36.
- [36] C. Feichtenhofer, A. Pinz, and A. Zisserman, "Convolutional two-stream network fusion for video action recognition," in *IEEE/CVF Conf. on Computer Vision and Pattern Recognition*, 2016, pp. 1933–1941.
- [37] J. Donahue, L. Anne Hendricks, S. Guadarrama, M. Rohrbach, S. Venugopalan, K. Saenko, and T. Darrell, "Long-term recurrent convolutional networks for visual recognition and description," in *IEEE/CVF Conf. on Computer Vision and Pattern Recognition*, 2015, pp. 2625–2634.
- [38] T.-W. Hui, X. Tang, and C. Change Loy, "Liteflownet: A lightweight convolutional neural network for optical flow estimation," in *IEEE/CVF Conf. on Computer Vision and Pattern Recognition*, 2018, pp. 8981–8989.
- [39] L. Fan, W. Huang, C. Gan, S. S. Ermon, B. Gong, and J. Huang, "End-to-end learning of motion representation for video understanding," in *IEEE/CVF Conf. on Computer Vision and Pattern Recognition*, 2018, pp. 6016–6025.
- [40] R. De Geest and T. Tuytelaars, "Modeling temporal structure with lstm for online action detection," in *IEEE Winter Conf. on Applications of Computer Vision*, 2018, pp. 1549–1557.
- [41] H. Ge, Z. Yan, W. Yu, and L. Sun, "An attention mechanism based convolutional lstm network for video action recognition," *Multimedia Tools and Applications*, vol. 78, no. 14, pp. 20 533–20 556, 2019.
- [42] R. Vemulapalli, F. Arrate, and R. Chellappa, "Human action recognition by representing 3d skeletons as points in a lie group," in *IEEE/CVF Conf. on Computer Vision and Pattern Recognition*, 2014, pp. 588–595.
- [43] M. Liu, H. Liu, and C. Chen, "Enhanced skeleton visualization for view invariant human action recognition," *Pattern Recognition*, vol. 68, pp. 346–362, 2017.
- [44] B. Fernando, E. Gavves, M. Jose´ Oramas, A. Ghodrati, and T. Tuytelaars, "Modeling video evolution for action recognition," in *IEEE Conf. on Computer Vision and Pattern Recognition*, 2015, pp. 5378–5387.
- [45] Yong Du, W. Wang, and L. Wang, "Hierarchical recurrent neural network for skeleton based action recognition," in *IEEE Conf. on Computer Vision and Pattern Recognition*, 2015, pp. 1110–1118.
- [46] K. C. Thakkar and P. J. Narayanan, "Part-based graph convolutional network for action recognition," in *British Machine Vision Conf.*, 2018.
- [47] Z. Yang, Y. Li, J. Yang, and J. Luo, "Action recognition with spatio-temporal visual attention on skeleton image sequences," *IEEE Trans. on Circuits and Systems for Video Technology*, vol. 29, no. 8, pp. 2405–2415, 2019.
- [48] S. Yan, Y. Xiong, and D. Lin, "Spatial temporal graph convolutional networks for skeleton-based action recognition," *ArXiv*, vol. abs/1801.07455, 2018.
- [49] J. C. Galloway, "Innovative approaches to promote mobility in children with cerebral palsy in the community," *Journal: Cerebral Palsy*, pp. 1–9, 2019.
- [50] D. J. Reinkensmeyer and M. L. Boninger, "Technologies and combination therapies for enhancing movement training for people with a disability," *Journal of NeuroEngineering and Rehabilitation*, vol. 9, no. 1, pp. 1–10, 2012.
- [51] J. Collins, J. Warren, M. Ma, R. Proffitt, and M. Skubic, "Stroke patient daily activity observation system," in *IEEE Int. Conf. on Bioinformatics and Biomedicine*, 2017, pp. 844–848.
- [52] A. Jaume-i Capó and A. Samcovi´c, "Vision-based interaction as an input of serious game for motor rehabilitation," in *IEEE Telecommunications Forum Telfor*, 2014, pp. 854–857.
- [53] A. Jaume-i Capó, P. Martínez-Bueso, B. Moya-Alcover, and J. Varona, "Interactive rehabilitation system for improvement of balance therapies in people with cerebral palsy," *IEEE Trans. on Neural Systems and Rehabilitation Engineering*, vol. 22, no. 2, pp. 419–427, 2013.
- [54] J. W. Burke, M. McNeill, D. Charles, P. Morrow, J. Crosbie, and S. McDonough, "Serious games for upper limb rehabilitation following stroke," in *IEEE Conf. in Games and Virtual Worlds for Serious Applications*, 2009, pp. 103–110.
- [55] J. C. Pulido, J. C. Gonzalez, C. Suarez-Mejías, A. Bandera, P. Bustos, and F. Fernandez, "Evaluating the child-robot interaction of the natherapist platform in pediatric rehabilitation," *Int. Journal of Social Robotics*, vol. 9, no. 3, pp. 343–358, 2017.
- [56] J. Redmon and A. Farhadi, "Yolov3: An incremental improvement," *ArXiv*, vol. arXiv:1804.02767, 2018.
- [57] T. Lin, M. Maire, S. J. Belongie, J. Hays, P. Perona, D. Ramanan, P. Dollár, and C. L. Zitnick, "Microsoft coco: Common objects in context," in *European Conf. on Computer Vision*, 2014.
- [58] K. He, X. Zhang, S. Ren, and J. Sun, "Deep residual learning for image recognition," in *IEEE/CVF Conf. on Computer Vision and Pattern Recognition*, 2016, pp. 770–778.
- [59] G. Farneback, "Two-frame motion estimation based on polynomial expansion," in *Scandinavian Conf. on Image analysis*. Springer, 2003, pp. 363–370.